# Enhanced Magnetic Properties of Polymer-Magnetic Nanostructures Synthesized by Ultrasonication

K. Thanigai Arul[a*], E. Manikandan[b-d*1], P. P. Murmu[e], J. Kennedy[c,e-f], M. Henini[c,g]

[a] Dept of Physics, AMET University, **Kanathur**-603 112, Tamil Nadu, **India**
[b] Dept of Physics, Thiruvalluvar University, TVUCAS Campus, **Thennangur**-604408, Tamil Nadu, **India**
[c] UNESCO-UNISA Africa Chair in Nanosciences-Nanotechnology, College of Graduate Studies, University of South Africa, Muckleneuk Ridge, PO Box 392, **Pretoria**, **South Africa**
[d] Central Research Lab, Bharath University, BIHER (Bharath Institute of Higher Education & Research), Selaiyur, Chennai 600073, Tamil Nadu, **India**
[e] National Isotope Centre, GNS Science, PO Box 31312, **Lower Hutt** 5010, **New Zealand**
[f] The MacDiarmid Institute for Advanced Materials and Nanotechnology, Wellington 6140, **New Zealand**
[g] School of Physics and Astronomy, Nottingham Nanotechnology and Nanoscience Center, University of Nottingham, Nottingham, NG7 2RD, **United Kingdom**

## Abstract

Polymer based nickel (Ni) and cobalt (Co) co-doped ferrites were prepared by adept ultrasonication route. Different concentrations of polymer [polyvinyl alcohol (PVA)] (0.2 g and 0.5 g) was added as a surfactant to the magnetic particles. The phase purity of Ni-Co ferrites (spinel structure) was confirmed by X-ray diffraction (XRD). Enhanced saturation magnetization of polymer based magnetic nanoparticles due to shape anisotropy and size. 0.2 wt% doped ferrite showed superparamagnetic characteristics with blocking temperature above room temperature. Hence, ultrasonication route is a rapid and effective technique for tailoring size and morphology of magnetic nanostructure that could be useful in magnetic-sensor applications.

**Keywords**: Ultrasonication; Magnetic Nanostructures; Polymers; Nanocomposites; Magnetization.

[1] * Corresponding: thanigaiarul.k@gmail.com; maniphysics@gmail.com; mani@tlabs.ac.za

## 1. Introduction

Nanosized particles possess distinct chemical and physical properties owing to their surface-to-volume ratio [1]. Generally, nanocomposites contain nanometric metals or metal oxide particles embedded in polymer matrices that provide a diverse range of magnetic and electrical properties. Cobalt ferrite ($CoFe_2O_4$) is a familiar hard magnetic material which has been widely studied due to its exciting magnetic properties [2]. However, nickel ferrite ($NiFe_2O_4$) is a soft ferrite which possesses low magneto-crystalline anisotropy but high electrical resistivity, and is used for power applications [3]. Inorganic ferrite materials were embedded in organic matrix for wide range of applications in electromagnetic interference (EMI), shielding [4-5], drug delivery [6] and magnetic resonance imaging (MRI) [7-10]. Various techniques have been suggested to synthesize nanophase materials such as mechanical milling [11], reversed micelles [12] and self-assembled monolayer [13]. Apart from above mentioned techniques, ultrasonication is a homogenizer to diminish particles size in a liquid to improve uniformity and stability. It is an efficient method to reduce the size of soft and hard magnetic particles. Dispersion and deagglomeration of particles in liquids are the significant application of ultrasonicator. Ultrasound can be employed to aid extraction, homogenization, freezing, crystallization, filtration and drying process [14]. Ultrasonication method has been employed in the prepared of uniform sized nanostructures of metals, metal oxides, graphene, and polymer nanocomposites for several applications.

Particle size, distribution of particles and morphology may not be controlled during conventional synthesis process. This could be solved by employing polymers, surfactants or capping agents. However, it is indistinguishable to comprehend the mechanism of variation in particle size, distribution and morphology of the particles. Polymers were coated on the surface of nanoparticles for protecting oxidation and to provide well controlled growth to tailor morphology of the nanoparticles. Nathani et al. reported the magnetic behavior of mechanical milling of nickel ferrite and polyethylene by in-situ polymerization of nickel ferrite polystyrene nanocomposites with core-shell morphology of particles [15]. Xiang et al. reported on polyvinyl pyrrolidone based cobalt–nickel ferrite nanofibers by electrospinning route. They found that the saturation magnetization and coercivity lie in the range 29.3–56.4 emu. $g^{-1}$ and 210–1255 $O_e$, respectively [16]. Zhang et al reported decrease in coercivity and increase in magnetization of $NiFe_2O_4$ magnetic nanorods via a Poly (ethylene glycol) PEG-assisted route [17]. Polyvinyl alcohol (PVA) is semi-crystalline, non-toxic, biocompatible,

biodegradable polymer with good chemical resistance which is employed for biomedical applications [18]. In literature, very few studies related to magnetic polymer nanocomposites via ultrasonication assisted technique are reported. Chitra et al. reported ultrasonication on polyaniline/$NiCoFe_2O_4$ which showed spherical morphology with increase in magnetic saturation [19]. However, to the best of our knowledge, no reports available on polyvinyl alcohol (PVA) based hard soft ferrites synthesized by ultrasonication route to examine physicochemical and magnetic properties.

## 2. Materials and Methods

Polymer based nickel-cobalt co-doped ferrites ($NiCoFe_2O_4$) was prepared by ultrasonication route using precursors such as ferric chloride (Merck), nickel (II) chloride hexahydrate (Merck), cobalt chloride hexahydrate and poly-vinyl alcohol (PVA) (CDH laboratory reagents). Solutions of $FeCl_3$ (0.4 M), $NiCl_2.6H_2O$ (0.1 M) and $CoCl_2.6H_2O$ (0.1 M) were mixed at 60 °C for 30 min. Subsequently, hydrazine hydrate is added drop wise to the solution which transformed into black colored solution. Final solution was ultrasonicated using Sonics-Vibra-Cell VCX (750W) 750 probe ultrasonicator with pulse time (three min) for 30 min. Ultimately, the solution was dried in hot air oven at 80 °C and grounded to obtain fine powders. Hereafter, it is referred as UNCF. The polymer (PVA) with different concentrations (0.2 gm and 0.5 gm) was added separately to Ni-Co ferrites solution to synthesize polymer based magnetic nanostructure and the samples are labeled as 0.2PUNCF and 0.5PUNCF, respectively.

## 3. Results and Discussion

### 3.1. XRD analysis

X-ray diffraction (XRD) of the samples was carried out using Bruker XRD $CuK_\alpha$ radiation (0.154 nm). Fourier transform infrared spectroscopy (FTIR) and Raman analysis of the samples were examined using BOMEMDA-8 FTIR and Jobin Yvon, respectively. The surface morphology was analyzed by scanning electron microscopy (SEM) (Carl Zeiss MA15/EVO18). Magnetic properties of the magnetic nanostructures were carried out by vibrating sample magnetometer (VSM) in a physical property measurement system (PPMS) from Quantum design.

The XRD patterns of (a) UNCF, (b) 0.2PUNCF and (c) 0.5PUNCF are shown in Fig. 1A. The major peaks are associated with (220), (311), (400), (422), (511) and (440) planes of $NiCoFe_2O_4$ using JCPDS (03-0864) and JCPDS (10-0325) values. The average crystallite size and lattice parameter were calculated using MAUD (Material Analysis Using Diffraction) software and the values are shown in Table 1. The crystallite size was around 105 nm for UNCF sample. The decrease in crystallite size was observed for 0.2PUNCF which could be due to high temperatures and pressures at microscopic level of the sonicated composite in colloidal solution by the formation of acoustic cavitation [20]. As the polymer incorporation increases to 0.5 wt% of PVA to UNCF, the crystallite size was enhanced which might be due to the increase in chemical activity of polymer chains. The chemical activity is increased by the acoustic cavitation by creating radical reactions in the solutions [19]. The lattice parameter decreased upon incorporation of polymer into Ni-Co ferrites. Wang et al. reported increased lattice parameter (8.366 Å) for $CoFe_2O_4$ and 8.342 Å for $NiFe_2O_4$ [3]. For 0.5PUNCF, the (220) plane is a prominent compared to other planes which could be due to growth kinetics plane directions. The intense (311) plane was attained for 0.2PUNCF. Ultrasonication and polymer incorporation change the growth rate which could modify the plane orientation as observed in 0.2PUNCF and 0.5PUNCF samples.

**3.2. FTIR**

FT-IR spectra of UNCF and 0.5PUNCF are shown in the Fig. 1B. A broad absorption band was observed between 3841 $cm^{-1}$ and 3200 $cm^{-1}$ which corresponds to O-H stretching band of complex metal-hydroxyl groups. The bands at 3435 $cm^{-1}$ and 1609 $cm^{-1}$ could be due to OH stretching vibration through hydrogen bonding in metal oxides. Adsorbed atmospheric $CO_2$ in trace level was confirmed by absorption peak at around 2367 $cm^{-1}$ which assigned to C=O stretching vibrations of carboxylate group of $CO_2$ gas. The peak at 1403 $cm^{-1}$ was attributed may be also due to adsorption of carbonate group [21]. The peak at 1200 $cm^{-1}$ is attributed to C-OH stretching vibrations [22]. The peak at 1380 $cm^{-1}$ is assigned to symmetric stretching of $CO_3^{2-}$ [23]. The peak at about 1560 is attributed to the $NH_2$ group may be due to hydrazine [24]. The Fe–O bond in tetrahedral and octahedral sites in $NiCoFe_2O_4$ was observed at 638 $cm^{-1}$.

**Table 1** Average crystallite size and lattice parameter of polymer based nickel and cobalt ions co-doped ferrites

| **Sample code** | **Crystallite size (nm)** | **Lattice parameter** |
|---|---|---|
| | | a=b=c (Å) |
| UNCF | 105 | 8.200 |
| 0.2PUNCF | 60 | 8.000 |
| 0.5PUNCF | 98 | 7.800 |

The metal oxygen band at 590 $cm^{-1}$ was observed which corresponds to intrinsic stretching vibration of metal at tetrahedral site. Cobalt ion substitution in spinel ferrites was observed at the peak 1087 $cm^{-1}$. The band of stretching mode of the metals was found to be in the range of 600–500 $cm^{-1}$ [12]. The bands in the range 600-500 $cm^{-1}$ and 1087 $cm^{-1}$ were suppressed upon addition of PVA into $NiCoFe_2O_4$ which confirmed the functionalization of Ni-Co ferrites with PVA by forming hydrogen bond [13].

### 3.3. Raman Analysis

Raman spectra of (a) UNCF, (b) 0.2PUNCF and (c) 0.5PUNCF are shown in Fig.1C. Five Raman active modes ($A_{1g} + E_g + 3F_{2g}$) are observed in Ni-Co ferrites. The less intense peak at 680 $cm^{-1}$ corresponds to symmetric stretching of oxygen atoms with Fe-O (and Ni-O) bonds in the tetrahedral sites. $E_g$ mode was observed at 320 $cm^{-1}$ which corresponds to symmetric bending mode of oxygen bonding to metal ions. The peaks at 480 $cm^{-1}$ and 530 $cm^{-1}$ are ascribed to asymmetric bending mode of oxygen [$F_{2g}(3)$] and asymmetric stretching mode of iron (nickel, cobalt) and oxygen [$F_{2g}(2)$] modes, respectively. Translational movement of tetrahedron [$F_{2g}(1)$] was observed at 210 $cm^{-1}$ [14,19]. Addition of polymer to Ni-Co ferrites, suppressed all four Raman modes and except the mode $F_{2g}(3)$ which confirmed surface functionalization of the polymer to metal oxides by forming hydrogen bonding. Raman modes of the polymer were observed at 1362 $cm^{-1}$ and 1604 $cm^{-1}$ which corresponding to C-H bending mode of polymer and the first-order scattering ($E_{2g}$ mode), respectively [25].

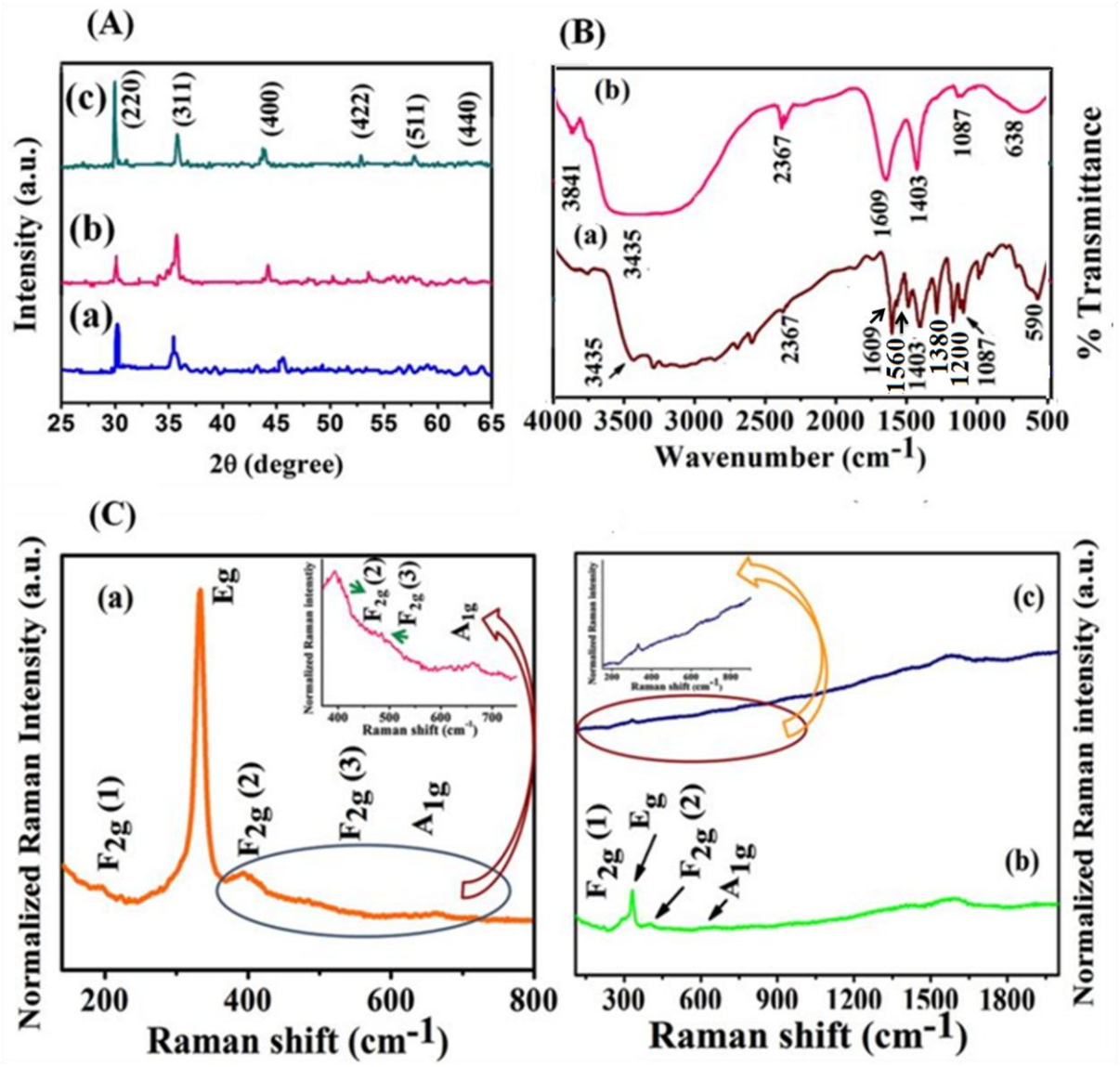


**Fig. 1A.** XRD patterns of (a) UNCF, (b) 0.2PUNCF and (c) 0.5PUNCF; **Fig.1B.** FTIR spectra of (a) UNCF and (b) 0.5PUNCF; **Fig. 1C.** Raman spectra of (a) UPNCF, (b) 0.2PUNCF and (c) 0.5PUNCF (inset of Fig. 3(c) is magnified portion of spectra from 200 $cm^{-1}$ to 900 $cm^{-1}$).

### 3.4. SEM Analysis

The SEM images of $NiCoFe_2O_4$ without and with polymer incorporation are shown in Fig. 2. Spherical nanoparticles of $NiCoFe_2O_4$ were in the range of 500 nm to 700 nm in the absence of polymer (PVA). Wang et al. reported the synthesis of cubical spinal $M^{II}Fe_2O_4$ (M = Co, Mn, Ni) with high crystalline structure at 10 min irradiation by microwave [26]. Addition of PVA into Ni-Co-ferrites and ultrasonication leads to modification of the morphology to self-assembled bead like patterns (Fig.2b). The size of beads was in the range 400-600 nm. The

formation of self-assembled bead could be due to the polymer and radical reaction in the solution by acoustic cavitation. At higher concentration (0.5 wt%) of PVA, rectangle (~100 nm × 300 nm) shaped morphology was observed which is due to the enhanced growth kinetics and chemical activity by acoustics (Fig.2c) [26-28]. $CoFe_2O_4$, nanocrystals can be prepared with a controlled shape of nearly spherical or cubic shape of the $CoFe_2O_4$. Shape is a dominating factor for the coercivity of nanocrystals because, of surface anisotropy [29]. PEG (Polyethylene glycol) with an ordered chain structure is adsorbed at the surface of metal oxide colloid and decreased its activities by the polymer [30]. The addition of PEG to the metal oxide colloids will change the kinetics of the growing colloids, which leads to anisotropic growth of the nanocrystals [31]. In the present case, while adding PVA to $NiCoFe_2O_4$, the morphology was modulated due to variation in growth kinetics of metal oxide, not only because of polymer but also by acoustic cavitations.

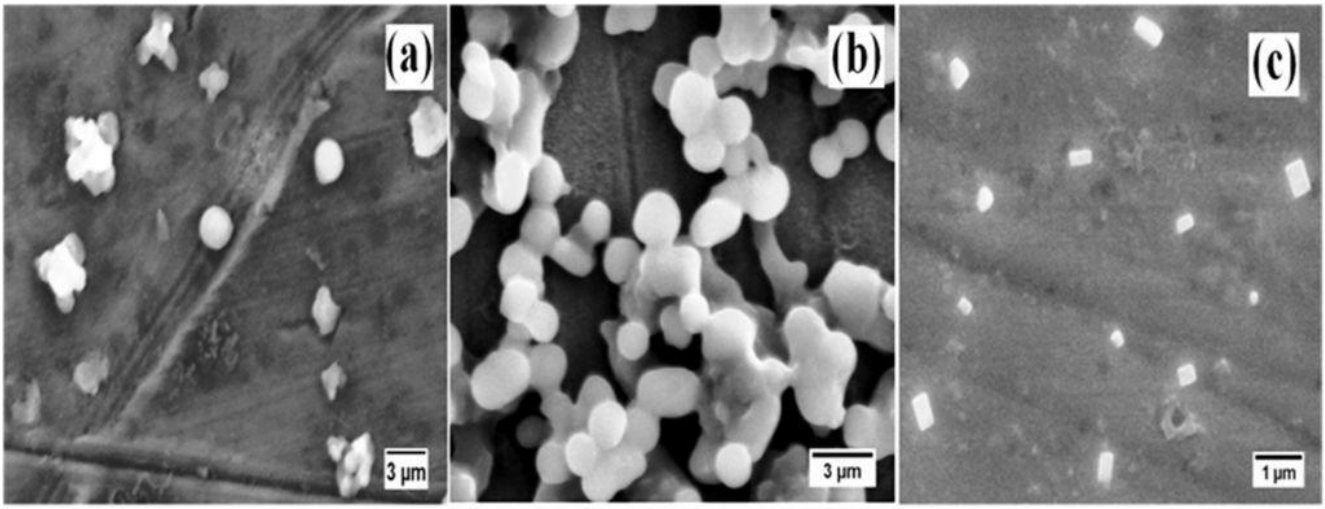


Fig. 2. SEM images of (a) UNCF, (b) 0.2PUNCF and (c) 0.5PUNCF

### 3.5. Magnetic measurements

Magnetic properties of UNCF, 0.2PUNCF and 0.5PUNCF were studied using vibrating sample magnetometer. Field dependent magnetization curves for UNCF, 0.2PUNCF and 0.5PUNCF at 300 K are shown in Fig.3. The UNCF and 0.5PUNCF showed paramagnetic behavior where magnetization increased with increasing the magnetic field. The 0.2PUNCF sample exhibited contribution from a ferromagnetic phase on top of paramagnetic signal. The saturation magnetization (Ms) of 0.2PUNCF was much higher than the 0.5PUNCF and UNCF samples. Enhanced saturation magnetization (Ms) of 0.2PUNCF compared to 0.5PUNCF and UNCF could be due to oxygen vacancies, spin exchange interaction and shape anisotropy [32]. Inset to the Fig. 3 illustrates the coercive magnetic field and remanent

magnetization (Mr). The coercivity and Mr for UNCF sample was 880 Oe and 0.02 emu/g respectively. For 0.2PUNCF coercivity and Mr for UNCF sample was 130 Oe and 0.01 emu/g correspondingly. The 0.5PUNCF showed similar Mr as to 0.2PUNCF but had a higher coercivity of 305 Oe. Decrease in coercivity by adding polymer to Ni-Co ferrites can be explained by domain structure, strains, crystalline anisotropy and shape anisotropy [33-34].

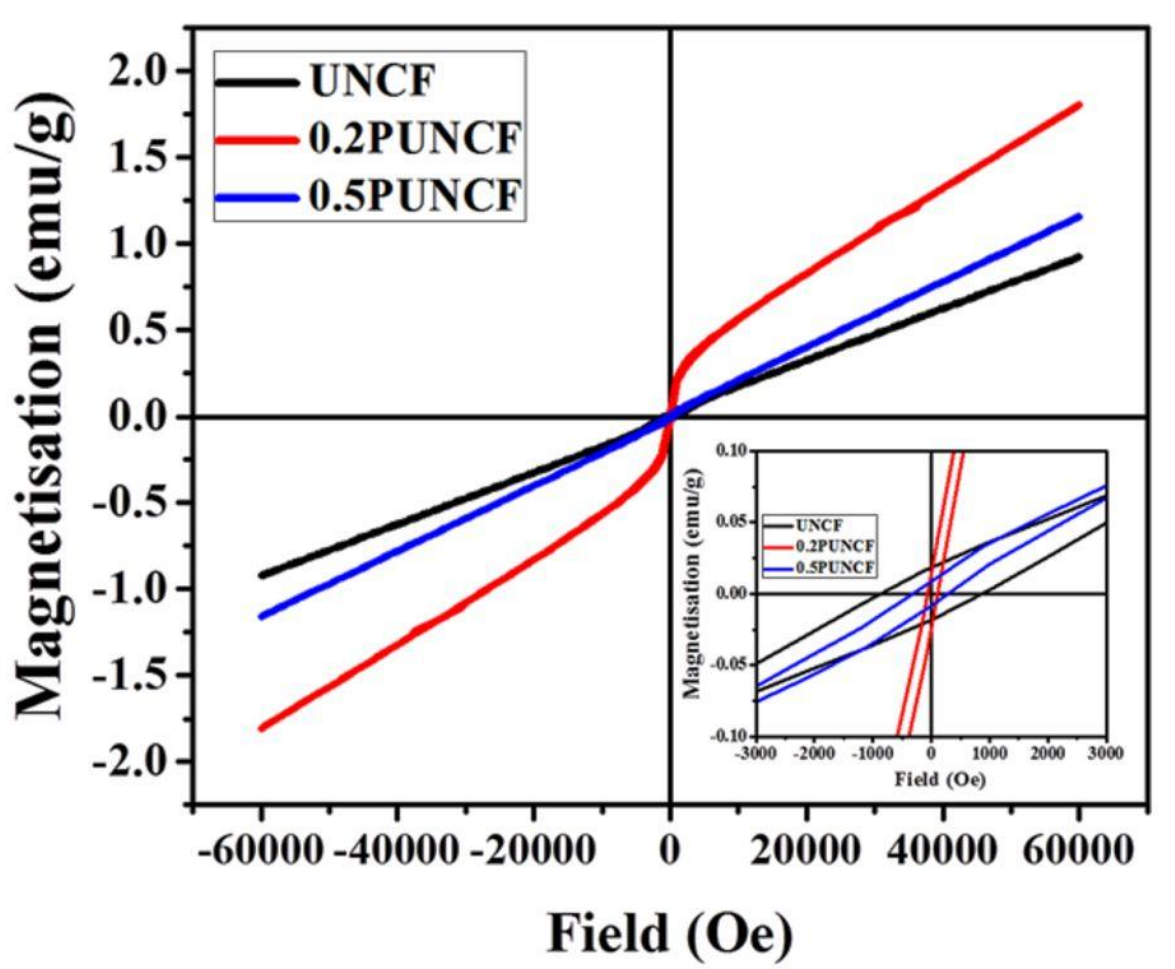


**Fig.3.** M (H) curves of (a) UNCF, (b) 0.2PUNCF and (c) 0.5PUNCF at 300 K (inset figure is magnified portion of M(H) from -3000 $O_e$ to 3000 $O_e$.

The presence of shape anisotropy can considerably enhance the magnetic properties of nanoparticles [35]. Shape, crystallinity and magnetization direction play significant role in determining the magnetic properties of the magnetic materials. At the surface of the grains, the modulation in cations coordination and breaking of bond may cause exchange fields as well as canting of spin or disorder in crystal field which activate surface anisotropy [36]. Wu et al. reported that the saturation magnetization reduces as cube sizes decreased due to increase in surface-to-volume ratio of nanoparticle and absorption of ligands. It affects the

electronic and magnetic structures at the surface and thus affects the magnetic properties of the material [37-38]. The magnetic anisotropy energy constant was increased with the reduction in particle size, due to the influence of surface anisotropy. At 0.2PUNCF, the size of self-assembled bead reduced which leads to enhance saturation magnetization by the impact of surface anisotropy. In elongated particles, the contribution of surface to the effective anisotropy leads to increase in the coercivity. The spin interactions are responsible for effective anisotropy which is contributed from shape anisotropy and surface magnetic spin [39]. Size effect and interconnected particles (0.2PUNCF) play a major to enhance the saturation magnetization and remanent magnetization rather than the increased particle size (UNCF) and elongated particles (0.5PUNCF).

Temperature dependent magnetization of UNCF, 0.2PUNCF and 0.5PUNCF at 100 Oe are shown in Fig. 4. Zero field cooled (ZFC) and field cooled (FC) curves of UNCF are shown in Fig.4a. Magnetic moment was decreased with increase in temperature for ZFC and FC (Fig.4a). At low temperatures the surface spin freeze in preferred orientation and moment saturate (0.012 emu/g) for ZFC in UNCF. However, at field cooled, the moment of UNCF was enhanced (0.0325 emu/g) could be rotation of the magnetization of the thermally hindered particles in the field direction. The trend followed the Curie's law for paramagnetic material where magnetization is affected by the temperature. The 0.5PUNCF sample showed similar trend as the UNCF sample where ZFC and FC decreased with increasing temperatures. However, the irreversibility in this sample was stronger than UNCF sample suggesting enhanced magnetic ordering in this system. On the contrary, 0.2PUNCF sample showed that the magnetization increased when the temperatures in increased up to 350 K. The FC curve followed Curie's law where magnetization decreased with lowering the temperatures. Similar trend was observed in superparamagnetic nanoparticles where sample showed hysteresis below blocking temperature [42-44]. At low temperatures (~32 K) of 0.2PUNCF (ZFC), the moment was decreased (0.0135 emu/g) may be due to blocking of particle moment in chaotic directions. The magnetic moment of 0.2PUNCF (ZFC) was enhanced with increase in temperature and it was saturated (0.0482 emu/g) above 350 K could be due to deliberate rotation of the magnetization of thermal hindered particles moment in the direction of field [40-41]. FC of 0.2PUNCF, the moment decreased with increase in temperature and at low temperature (5 K), it increased to 0.102 emu/g. On adding polymer (0.5 wt%) to Ni-Co ferrites, ZFC and FC were also reduced with increase in temperature. At low temperatures (~25 K), the moment of 0.5PUNCF was found to be 0.040 emu/g in both

ZFC and FC. Surface anisotropy in 0.2PUNCF sample leads to high magnetization and low coercivity consistent with the magnetic properties of superparamagnetic nanoparticles [42-48].

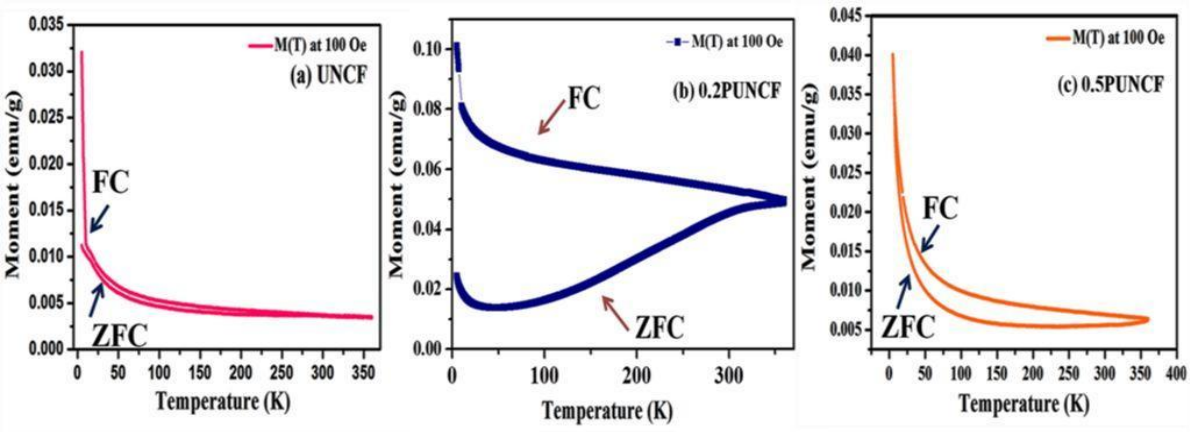


**Fig.4.** Zero field cooled (ZFC) and field cooled (FC) curves of (a) UNCF and (b) 0.2PUNCF and (c) 0.5PUNCF.

## 4. Conclusion

Magnetic polymer nanostructures of $NiCoFe_2O_4$/PVA have been prepared via an in-situ ultrasonication process. The samples were characterized by XRD, FTIR, Raman and SEM analyses respectively. In addition, magnetic properties were also investigated by VSM. XRD analysis confirmed the phase purity of Ni-Co ferrites (spinel structure). Reduced average crystallite size by 42.8% of Ni-Co ferrites was attained upon polymer incorporation. At 0.2 wt% of polymer, self-assembled beads of magnetic particles were observed whereas, for 0.5PUNCF, rectangle shaped was attained. Enhanced magnetic properties of polymer (0.2 wt%) incorporated in Ni-Co ferrite were observed due to size and shape anisotropy. The field and temperature dependent magnetization results showed superparamagnetic behavior in 0.2 wt% doped ferrite. Collectively, ultrasonication route is a simple, robust and cost-effective route to tailor the morphology of magnetic structures and creating size and shape anisotropy for enhancing magnetic properties. Hence, polymer based magnetic nanostructures could be useful in magneto-sensors and magnetic hyperthermia applications.


## Acknowledgement

The authors (K.T & E.M) thanks to National Isotope Centre, GNS Science, Lower Hutt, New Zealand and Prof. M. Maaza, iThemba LABS, South Africa for providing characterization facilities.

## References


1. P Ball, G. Li, Science at the atomic scale, Nature 355 (1992) 761–766.
2. M.A. Amer, A. Tawfik, A.G. Mostafa, A.F.E. Shora, S.M. Zaki, Spectral studies of Co substituted Ni–Zn ferrites, J. Magn. Magn. Mater. 323 (2011) 1445–1452.
3. A. Manikandan L.J. Kennedy, M. Bououdina, J.J. Vijaya, Microwave combustion synthesis, structural, optical and magnetic properties of $Zn_{1-x}Sr_xFe_2O_4$ nanoparticles, Ceram. Inter. 39 (2013) 5909-5917.
4. J. Slama, A. Gruskova, R. Vicen, S. Vicenova, R. Dosoudil, J. Franek, Composite material with substituted Li ferrite for high-frequency applications, J. Magn. Magn. Mater. 254 (2003) 642–645.
5. R.P. Pant, R. Rashmi, M. Krishna, P.S. Negi, K. Ravat, U. Dhawan, S.K. Gupta, D.K. Suri, XRD, SEM, EPR and microwave investigations of ferrofluid-PVA composite films, J. Magn. Magn. Mater. 149 (1995) 10–13.
6. A. Manikandan, L.J. Kennedy, M. Bououdina, J.J. Vijaya, Synthesis, optical and magnetic properties of pure and Co-doped $ZnFe_2O_4$ nanoparticles by microwave combustion method, J. Magn. Magn. Mater. 349 (2014) 249–258.
7. S.A.G. Lopera, R.C. Plaza, A.V. Delgado, Synthesis and Characterization of Spherical Magnetite/Biodegradable Polymer Composite Particles, J. Colloid Interface Sci. 240 (2001) 40–47.
8. P. Pulisova, J. Kovac, A. Voigt, P. Raschman, Structure and magnetic properties of Co and Ni nano-ferrites prepared by a two-step direct microemulsions synthesis, J Magn Magn Mater. 341 (2013) 93–99.
9. X. Jia, D.R. Chen, X.L. Jiao, T. He, H.Y. Wang, W. Jiang, Monodispersed Co, Ni-Ferrite Nanoparticles with Tunable Sizes: Controlled Synthesis, Magnetic Properties, and Surface Modification, J. Phys. Chem. C. 112 (2008) 911–917.
10. M.C.K. Wiltshire, J.B. Pendry, I.R. Young, D.J. Larkman, D.J. Gilderdale, J.V. Hajnal, Microstructured magnetic materials for RF flux guides in magnetic resonance imaging, Sci. 291 (2001) 849–851.
11. A. Corrias, G. Ennas, A. Musinu, G. Paschina, D. Zedda, Iron-silica and nickel-silica nanocomposites prepared by high energy ball milling, J. Mater. Res. 12 (1997) 2767–2772.

12. M.P. Pileni, I. Lisiecki, Nanometer metallic copper particle synthesis in reverse micelles, Colloid Surf A, 80 (1993) 63–68.
13. C. Yee, G. Kataby, A. Ulman, T. Prozorov, H. White, A. King, M. Rafailovic, J. Sokolov, A. Gedanken, Self-assembled monolayers of alkanesulfonic and -phosphonic acids on amorphous iron oxide nanoparticles, Langmuir, 15 (1999) 7111–7115.
14. T.J. Mason, L. Paniwnyk, J.P. Lorimer, The uses of ultrasound in food technology, Ultrason. Sonochem. 3 (1996) S253–S260.
15. H. Nathani, R.D.K. Misra, Surface effects on the magnetic behavior of nanocrystalline nickel ferrites and nickel ferrite-polymer nanocomposites, Mater. Sci. Eng. B.113 (2004) 228–235.
16. J. Xiang, Y. Chu, X. Shen, G. Zhou, Y. Guo, Electrospinning preparation, characterization and magnetic properties of cobalt-nickel ferrite ($Co(1-x)Ni(x)Fe_2)O_4$) nanofibers, J Colloid Interface Sci. 376 (2012) 57–61.
17. D.E. Zhang, X.J. Zhang, X.M. Ni, H.G. Zheng, D.D. Yang, Synthesis and characterization of $NiFe_2O4$ magnetic nanorods via a PEG-assisted route, J. Magn Magn. Mater. 292 (2005) 79–82.
18. S. Mirzaee, S.F. Shayesteh, S. Mahdavifar, Anisotropy investigation of cobalt ferrite nanoparticles embedded in polyvinyl alcohol matrix: A Monte Carlo study, Polym. 55 (2014) 3713–3719.
19. P. Chitra, A. Muthusamy, R. Jayaprakash, E.R. Kumar, Effect of ultrasonication on particle size and magnetic properties of polyaniline $NiCoFe_2O_4$ nanocomposites, J. Magn. Magn. Mater. 366 (2014) 55–63.
20. S.J. Doicrycz, K.S. Suslick, Interparticle collisions driven by ultrasound, Science 247 (1990) 1067–1069.
21. L.F. Koroleva, L.P. Larionov, N.P. Gorbunova, Biomaterial Based on Doped Calcium Carbonate-Phosphate for Active Osteogenesis, J. Biomater. Nanobiotech. 3 (2012) 226-237.
22. M.E. Uddin, N.H. Kim, T. Kuila, S.H. Lee, D. Hui, J.H. Lee, Preparation of reduced graphene oxide-$NiFe_2O_4$ nanocomposites for the electrocatalytic oxidation of hydrazine, Composites Part B 79 (2015) 649–659.

23. A. Anzlovar, M. Marinsek, Z.C. Orel, M. Zigon, Basic zinc carbonate as a precursor in the solvothermal synthesis of nano zinc oxide, Mater. Des. 86, (2015) 347–353.

24. M. Menelaou, K. Georgoula, K. Simeonidis, C.D. Samara, Evaluation of nickel ferrite nanoparticles coated with oleylamine by NMR relaxation measurements and magnetic hyperthermia, Dalton Trans. 43 (2014) 3626-3636.

25. A. Martinelli, A. Matic, P. Jacobsson, L. Borjesson, M.A. Navarra, A. Fernicola, S. Panero, B. Scrosati, Structural analysis of PVA-based proton conducting membranes, Solid State Ionics, 177 (2006) 2431–2435.

26. W.W. Wang, Microwave-induced polyol-process synthesis of M"$Fe_20_4$ (M = Mn, Co) nanoparticles and magnetic property, Mater. Chem. Phys. 108 (2008) 227–231.

27. A. Pradeep, P. Priyadharsini, G. Chandrasekaran, Production of single phase nano size $NiFe_2O_4$ particles using sol–gel auto combustion route by optimizing the preparation conditions, Mater. Chem. Phys. 112 (2008) 572–576.

28. K. Oya, T. Tsuru, Y. Teramoto, Y. Nishio, Nanoincorporation of iron oxides into carrageenan gels and magnetometric and morphological characterizations of the composite products, J. Polym. 45 (2013) 824–833.

29. Q. Song, Z.J. Zhang, Shape control and associated magnetic properties of spinel cobalt ferrite nanocrystals, J. Am. Chem. Soc. 126 (2004) 6164–6168.

30. J. Dobryszycki, S. Biallozor, On some organic inhibitors of zinc corrosion in alkaline media, Corros. Sci. 43 (2001) 1309–1319.

31. X.H. Liu, J. Yang, L. Wang, X.J. Yang, L.D. Lu, An improvement on sol-gel method for preparing ultrafine and crystallized titania powder, Mater. Sci. Eng. A.289 (2000) 241–245.

32. E. Iizuka, The Effects of Magnetic Fields on the Structure of Cholesteric Liquid Crystals of Polypeptides, J. Polym.4 (1973) 401–408.

33. K. Kuroiwa, Y. Koga, Y. Ishimaru, T. Nakashima, H. Hachisako, S. Sakurai, Morphological control of hybrid amphiphilic poly(N-isopropylacrylamide)/metal cyanide complexes, J. Polym. 48 (2016) 729–739.

34. A.B. Nawale, N.S. Kanhe, K.R. Patil, S.V. Bhoraskar, V.L. Mathe, A.K. Das, Magnetic properties of thermal plasma synthesized nanocrystalline nickel ferrite ($NiFe_2O_4$). J. Alloys Compd. 509 (2011) 4404–4413.

35. D.L.L. Pelecky, R.D. Rieke, Magnetic Properties of Nanostructured Materials, Chem. Mater. 8 (1996) 1770–1783.
36. E. Manova, B. Kunev, D. Paneva, I. Mitov, L. Petrov, C. Estournes, C.S. D'Orléan, J.L. Rehspringer, Mechano-Synthesis, Characterization, and Magnetic Properties of Nanoparticles of Cobalt Ferrite, $CoFe_2O_4$, Chem. Mater.16 (2004) 5689–5696.
37. N. Wu, L. Fu, M. Su M. Aslam, K.C. Wong, V.P. Dravid, Interaction of Fatty Acid Monolayers with Cobalt Nanoparticles, Nano Lett.4 (2004) 383–386.
38. R.H. Kodama, A.E. Berkowitz, E.J. McNiff Jr, S. Foner, Surface Spin Disorder in $NiFe_2O_4$ Nanoparticles, Phys. Rev. Lett. 77 (1996) 394–397.
39. F. Bodker, S. Morup, S. Linderoth, Surface effects in metallic iron nanoparticles, Phys Rev Lett.72 (1994) 282–285.
40. M.A. Gabal, Y.M.A. Angari, M.W. Kadi, Structural and magnetic properties of nanocrystalline $Ni_{1-x}Cu_xFe_2O_4$ prepared through oxalates precursors, Polyhedron, 30 (2011) 1185–1190.
41. S.H. Hosseini, R. Rahimi, H. Kerdari, Preparation of a nanocomposite of magnetic, conducting nanoporous polyaniline and hollow manganese ferrite, J. Polym. 43 (2011) 745–750.
42. H. Sawada, T. Kijima, M. Mugisawa, Selective preparation of novel fluoroalkyl end-capped co-oligomeric nanocomposite-encapsulated magnetites and magnetite-adsorbing co-oligomeric nanoparticles, J. Polym. 42 (2010) 494–500.
43. J. Kennedy, J. Leveneur, Y. Takeda, G.V.M. William, S. Kupke, D.R.G. Mitchell, A. Markwitz, J.B. Metson, Evolution of the structure and magneto-optical properties of ion beam synthesized iron nanoclusters, J. Mater. Sci. 47 (2012) 1127–1134.
44. J. Leveneur, J. Kennedy, G.V.M. Williams, J.B. Metson, Enhancement of the magnetic properties of iron nanoparticles upon incorporation of samarium, Appl. Phys. Lett. 98 (2011) 053111.
45. C. Sasikala, N. Durairaj, I. Baskaran, B. Sathyaseelan M. Henini E. Manikandan, Transition metal titanium (Ti) doped LaFeO3 nanoparticles for enhanced optical structural and magnetic properties. J. Alloys & Compounds. 712 (2017) 870–877.
46. T. Siva, S. Muralidharan, S. Sathiyanarayanan, E. Manikandan, M. Jayachandran. Enhanced Polymer Induced Precipitation of Polymorphous in Calcium Carbonate: Calcite Aragonite Vaterite Phases. J. Inorganic & Organometallic Polymers & Materials 27 (2017) 770-778.

47. A Diallo, TB Doyle, BM Mothudi, E Manikandan, V Rajendran, M Maaza. Magnetic behavior of biosynthesized $Co_3O_4$ nanoparticles. J. Magn. & Magn. Mater. 424 (2017) 251-255.
48. K Thanigai Arul, E Manikandan, R Ladchumananandasivam, M Maaza. Novel polyvinyl alcohol polymer based nanostructure with ferrites co- doped with nickel and cobalt ions for magneto- sensor application. Polymer International 65 (2016) 1482-1485.

**Graphical Abstract (for review)**

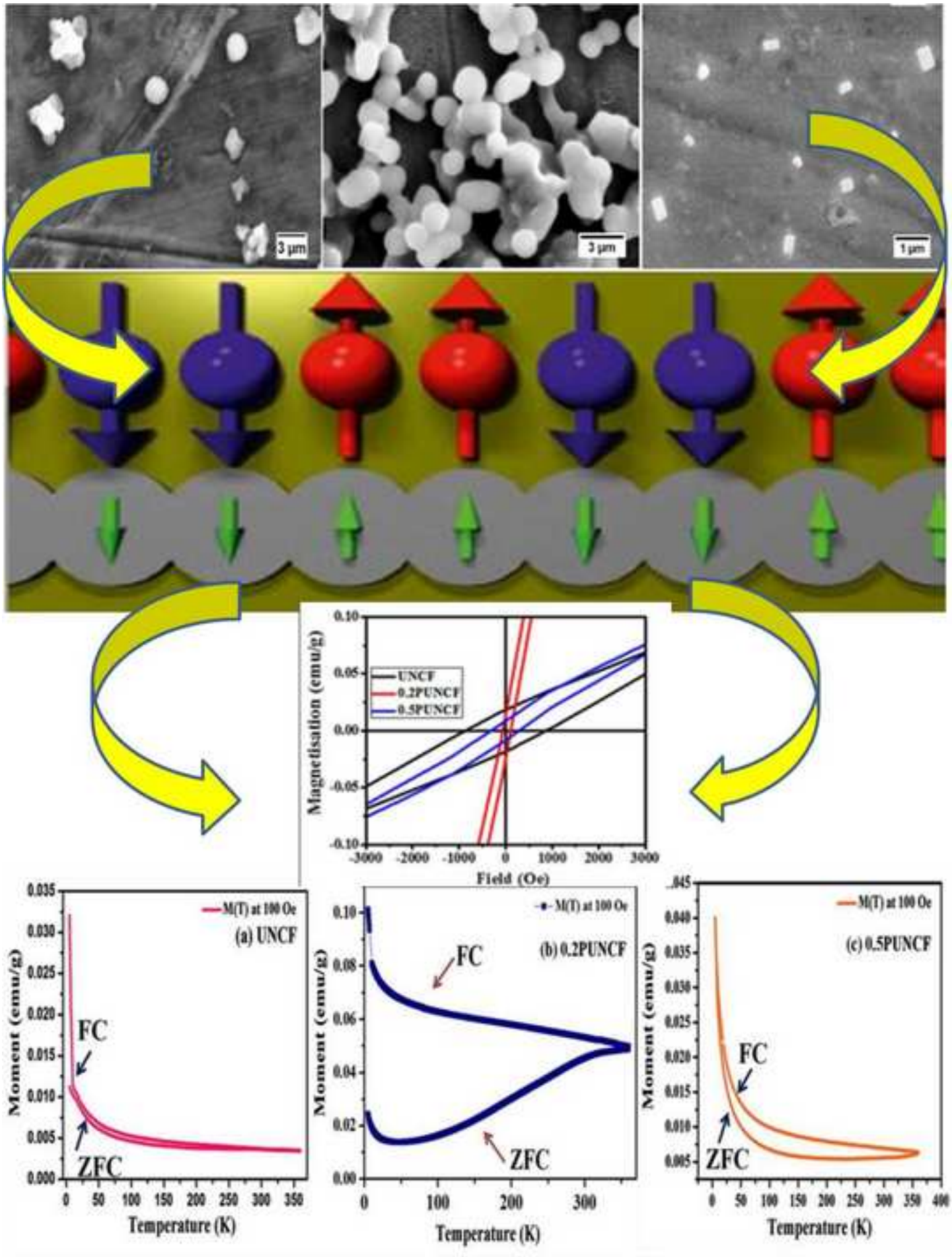

# HIGHLIGHTS

- Ultrasonication Technique Simple Rapid and Effective for Polymer Nanocomposites (NCs)
- Ni and Co ferrites doped to Polymer NCs with Different Concentrations
- Polymer [polyvinyl alcohol (PVA)] (0.2g and 0.5g) added as a Surfactant to Ferrites Materials
- Phase purity of Ni-Co ferrites (spinel structure) confirmed by XRD, FTIR, Raman techniques
- Enhanced Saturation Magnetization of Polymer NCs Magnetic NPs Shape Anisotropy and Size
- Polymer NCs Magnetic Materials useful for future Magnetic-Sensor Applications.

**List of table:**

**Table 1** Average crystallite size and lattice parameter of polymer based nickel and cobalt ions co-doped ferrites

| **Sample code** | **Crystallite size (nm)** | **Lattice parameter** a=b=c (Å) |
|---|---|---|
| UNCF | 105 | 8.200 |
| 0.2PUNCF | 60 | 8.000 |
| 0.5PUNCF | 98 | 7.800 |

Figure

Click here to download high resolution image

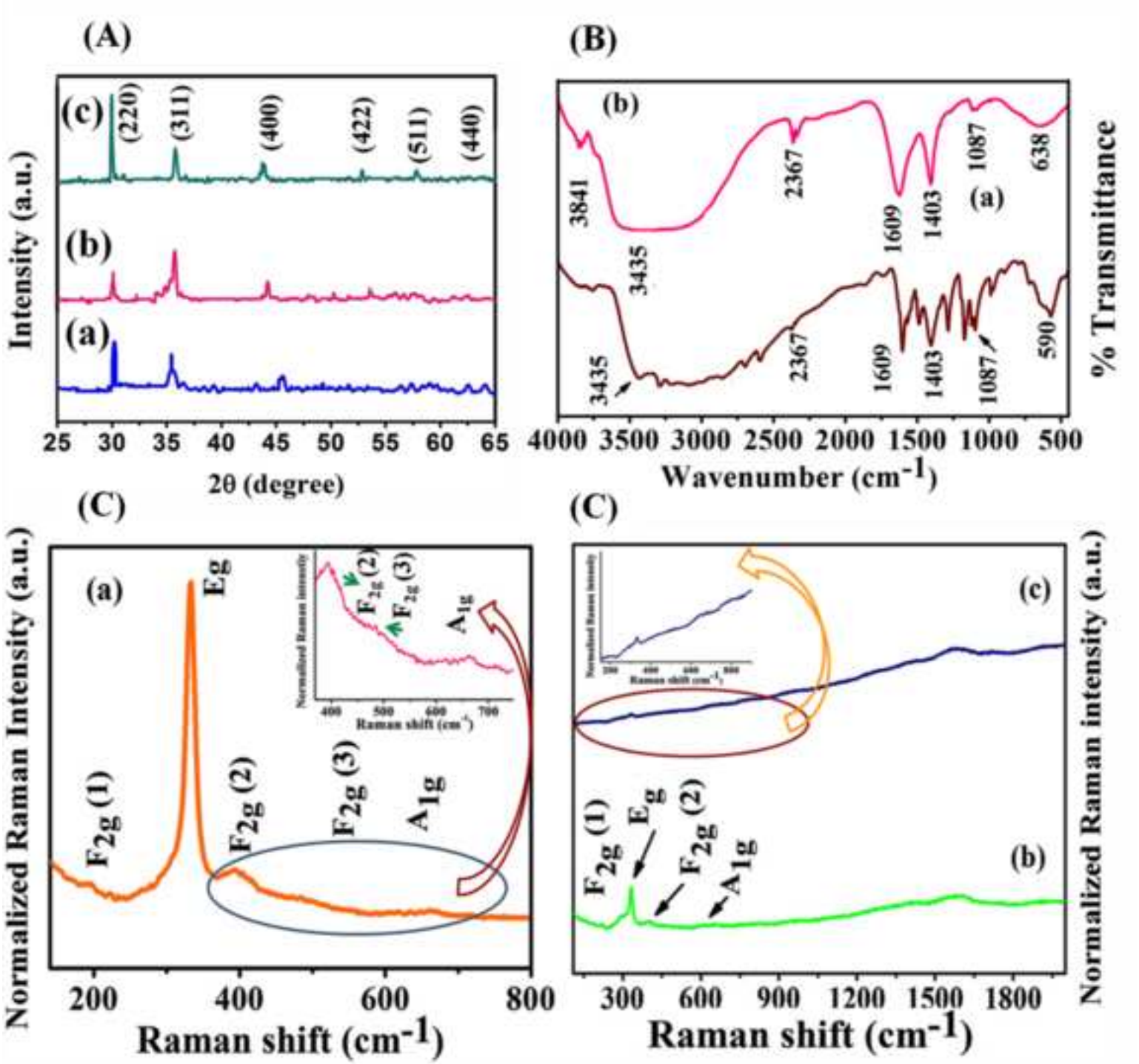

Figure
Click here to download high resolution image

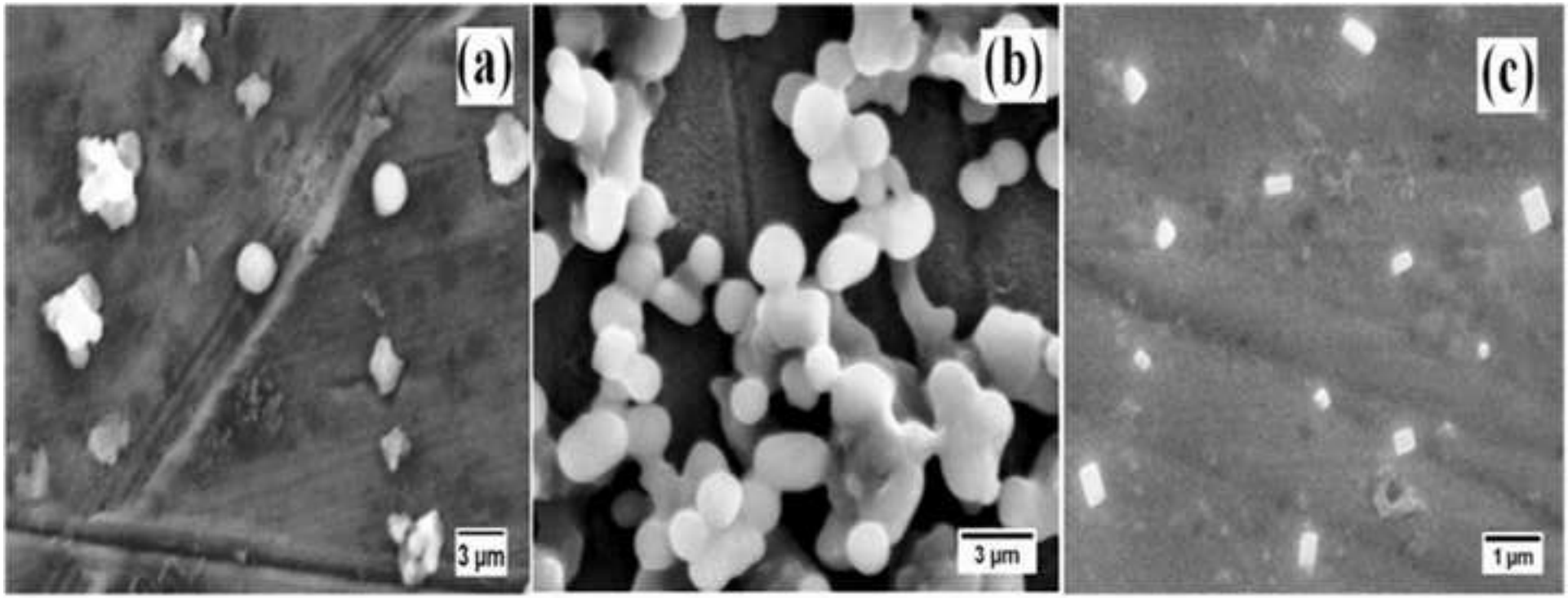

Figure

Click here to download high resolution image

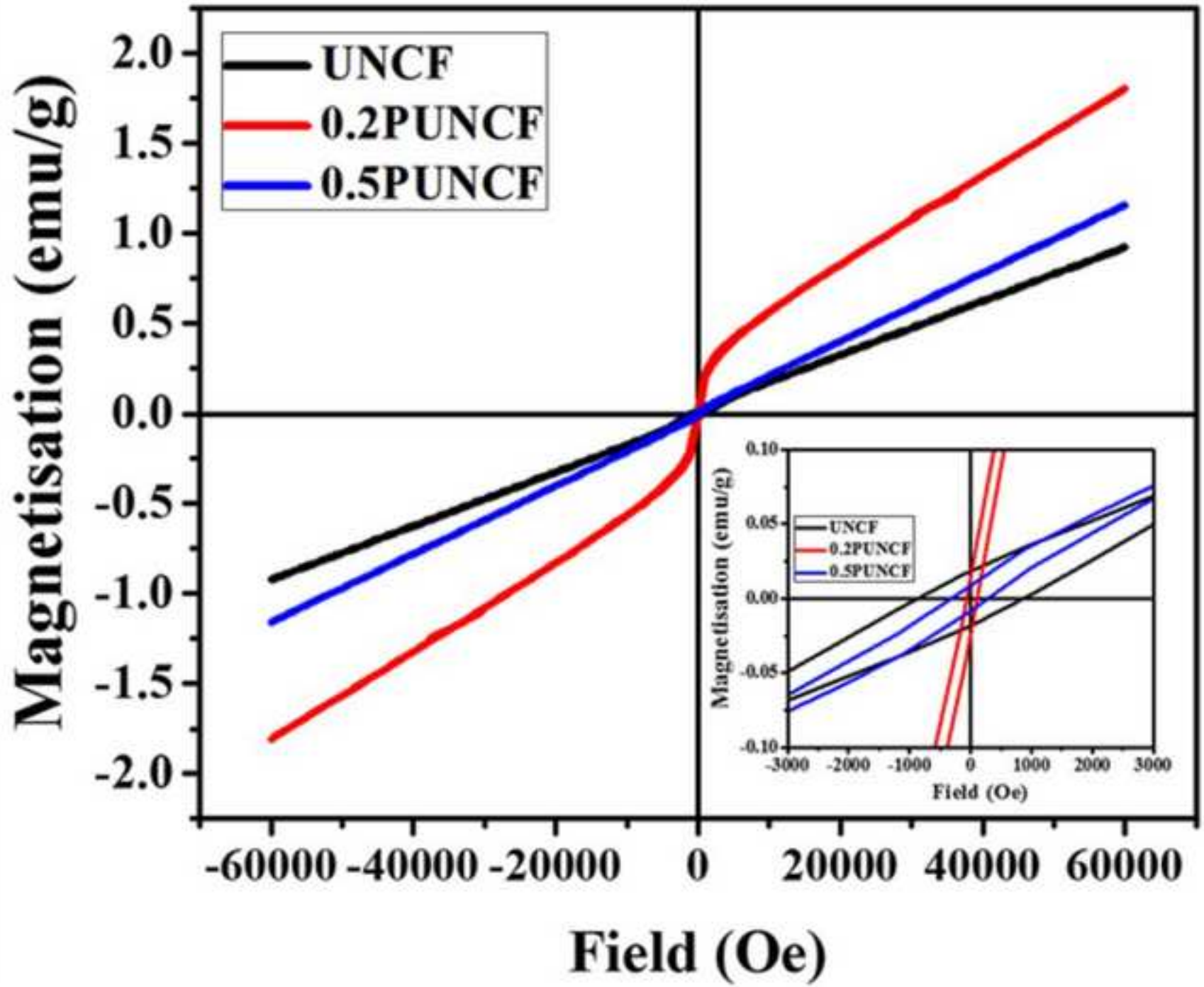

Figure

Click here to download high resolution image